Equal-efficiency diffraction of unpolarized wideband light with acousto-optic filters

Samuel Dupont, Justine Champagne, Jean-Claude Kastelik

Equal-efficiency diffraction of unpolarized wideband light with acousto-optic filters

Samuel Dupont[a]*; Justine Champagne[a] and J.C. Kastelik[a]

[a]*Univ. Polytech. Haut-de-France, CNRS, Univ. Lille, Centrale Lille, UMR 8520 - IEMN, F-59313 Valenciennes, France;*

[b]*INSA Hauts-de-France, F-59313 Valenciennes, France;*

Samuel.dupont@uphf.fr *corresponding author

Samuel Dupont, Professor at Université Polytechnique Hauts-de-France

UPHF

Campus Mont-Houy

59313 Valenciennes cedex 9

France

+33(0)3 27 51 14 42

Funding Information. National Research Agency, ANR
(grant ANR-17-CE04-0008 SPIT-FIRE)

Peranent reference to this article: https://doi.org/10.1080/09500340.2022.2085336

Equal-efficiency diffraction of unpolarized wideband light with acousto-optic filters

We present the diffraction of unpolarized light over a broad wavelength range using paratellurite Acousto-Optic Tunable Filters. The diffraction of unpolarized light usually relies on a specific operating point that is sensitive to the wavelength and angle of incidence, resulting in an operating ability over a narrow bandwidth. We present a detuning strategy to eliminate the angular dependence and obtain equal diffraction efficiency for both the linear polarization states over a broad bandwidth. We explain how to find the optimum operating frequency and present its dependency as a function of the wavelength. With the quasi-phase matching condition presented, the diffraction of unpolarized light over the 400 nm to700 nm band is possible with an efficiency of over 80%.

Keywords: acousto-optic devices; wavelength filtering devices; birefringence; polarization-selective devices

Subject classification codes: 230.1040; 230.7408; 260.1440; 130.5440

Introduction

Acousto-Optic (AO) devices have multiple uses including frequency shifters, modulators, deflectors, or filters [1–5]. Acousto-Optic Tunable Filters (AOTFs) are commonly used to measure the spectral composition of a light source [6]. They can also split an unpolarized beam into two orthogonal linear polarized beams [7]. Knowledge and control of the polarization state of an optical beam are of crucial importance in applications such as sensing [8-10] or laser beam modulation [11]. When combined with an imaging system, the ability to analyse the polarization can provide important information about the object observed [12, 13] and it is beneficial in various applications including biomedical analysis [14], the military sector to detect targets and mines [15], or environmental sciences and agriculture to provide information about plants and crops [16, 17].

The diffraction of unpolarized light using AOTFs, which can be used to analyse linear polarization, is possible over a limited wavelength range as the diffraction efficiency is wavelength-sensitive at a given incident angle [7]. Indeed, in birefringent acousto-optic crystals, an unpolarized input beam is divided into two orthogonally polarized beams. The simultaneous interaction of these two beams with the same efficiency is possible at a given wavelength for one incident angle and one operating frequency. These two parameters constitute the "Double Diffraction" (DD) operating point. When the wavelength is changed, a new incident angle-interaction frequency pairing must be determined but when a polychromatic incident beam is analysed, maintaining a fixed incident angle can be necessary for practical reasons. Consequently, as the wavelength of interest moves away from the operating point wavelength corresponding to the incident angle chosen, the more the interaction efficiency of the two polarization states differs. Hence with polychromatic light, knowledge of the polarization state of the incident beam is normally only possible over a very limited wavelength band.

In this paper, we analyse theoretically the characteristics of simultaneous diffraction over a wide optical range when a fixed incident angle is considered. In this configuration, we determined the conditions to maintain equal diffraction efficiencies without the need for realignment. To reach this goal, we optimized the choice of the acoustic operating frequency and the wavelength, which determines the initial incident angle. First, we show that for each optical wavelength there is one acoustic frequency corresponding to interaction efficiencies that are equivalent for the two polarization states. We then show that equal-efficiency Double Diffraction of unpolarized wideband light is possible by carefully choosing the initial incident angle. The properties of paratellurite (TeO2) and the slow shear wave were taken into consideration in our

calculations because numerous commercially available devices are based on this highly efficient configuration.

Simultaneous diffraction of unpolarized light

The acousto-optic diffraction efficiency can be very high under the Bragg phase-matching condition, the latter being dependent on the incident angle, the acoustic frequency, and the optical wavelength. The efficiency depends on the nature of the crystal (material properties and device geometry) and adherence to phase-matching conditions. In practice, for a given AOTF design, the diffraction efficiency for an optical wavelength λ depends on the optical incident angle θ_i and the acoustic frequency f.

In birefringent crystals, an efficient anisotropic acousto-optic interaction is possible. In such crystals, two propagation modes exist that correspond to the well-known “ordinary” and “extraordinary” rays. Two types of anisotropic diffraction can thus occur, one from the extraordinary to the ordinary ray (e→o) and the other from the ordinary to the extraordinary ray (o→e). From a theoretical point of view, one of the two diffraction types can be selected by adjusting the characteristics of the incident light: polarization state and direction of propagation (i.e. incident angle). When the incident optical wave is unpolarized, the two diffraction types generally occur at two different frequencies. Nevertheless, simultaneous diffraction of both linear polarization states with equal efficiency is possible at a very specific operating point (see [7] for a detailed description). In the latter case, there is “Double Diffraction” [10] with two diffracted light beams at the crystal output, as well as potentially a transmitted light beam (that fades out under appropriate acoustic power), as illustrated in figure 1. The two simultaneously diffracted beams are orthogonally polarized. The vector diagram corresponding to this special case is represented in figure 2. The diagram illustrates that

Double Diffraction (DD) is possible for a unique acoustic vector K and a particular incident angle θ_i. K is proportional to the acoustic frequency and so the vector diagram can be used to determine the interaction parameter values.

Figure 3 depicts the evolution of the interaction frequency as a function of the incident angle for the two anisotropic diffraction cases for a slow wave in a TeO_2 crystal. As can be seen, the (e→o) and (o→e) curves intersect at a single operating point specific to the wavelength λ considered. The coordinates of one of these points define the wavelength-sensitive DD point: ($f_{DD}(\lambda)$, $\theta_{DD}(\lambda)$). At this operating point, the exact phase-matching condition (synchronism) is respected simultaneously for the two diffraction types and the efficiencies of both interactions are identical and maximum for the wavelength λ considered. From 400 nm to 700 nm, the DD frequency can evolve over an operating range of 86 MHz and the incident angle over 0.15°. From figure 3, it is clear that when the incident angle is no longer $\theta_{DD}(\lambda)$, the curves corresponding to (e→o) and (o→e) split from one another. Hence, the synchronism conditions for each interaction are obtained with two different frequencies. Similarly, when the frequency is no longer $f_{DD}(\lambda)$, the synchronism conditions for each interaction are obtained with two different incident angles. Finally, when the optical wavelength is changed, large variations in the efficiency are observed as the DD parameters are significantly different, as illustrated for three different wavelengths in figure 1.

Consequently, the case of Double Diffraction for one wavelength can only be achieved for one specific parameter pairing: the acoustic interaction frequency (proportional to K) and the incident angle [7]. As it is considered that the third parameter, the optical wavelength, depends on the characteristics of the incident light to be analysed, these characteristics cannot be tuned experimentally. However, when considering wideband diffraction, the variation in the refractive index, n, as a function

of the wavelength has to be taken into account: the optical wave vector loci are inversely proportional to n. The Sellmeier formulas are introduced to deal with wavelength dependence [19]:

$$n_o = \sqrt{1 + \frac{2.5844\,\lambda^2}{\lambda^2 - 0.1342^2} + \frac{1.1557\,\lambda^2}{\lambda^2 - 0.2638^2}}$$

$$n_e = \sqrt{1 + \frac{2.8525\,\lambda^2}{\lambda^2 - 0.1342^2} + \frac{1.5141\,\lambda^2}{\lambda^2 - 0.2631^2}}$$

Figure 4 illustrates the vector diagram when the exact Bragg conditions are not met. In Figure 4a, an offset from the Bragg angle of incidence is depicted. As can be seen, a momentum mismatch, Δk, is introduced. In Figure 4b, Δk results from a change in the optical wavelength which modifies the wave vector loci. The momentum mismatch value is deduced from the wave vector loci and geometrical considerations.

Efficiency of simultaneous diffraction of unpolarized light

The analysis of the phase-matching conditions leads to an expression for the evolution of the diffraction efficiencies when the operating point departs from the exact Bragg conditions: the momentum mismatch Δk leads to a phase mismatch $\Delta\Phi$ = w* Δk that affects the interaction efficiency. The diffraction efficiency η was evaluated using the well-known formula [7]:

$$\eta = \frac{P}{P_0} \frac{\sin^2\left(\frac{\pi}{2}\sqrt{\frac{P}{P_0} + \left(\frac{\Delta\Phi}{\pi}\right)^2}\right)}{\frac{P}{P_0} + \left(\frac{\Delta\Phi}{\pi}\right)^2} \qquad (1)$$

Where P is the power of the acoustic wave, P_0 is the power required to obtain maximum efficiency, and $\Delta\Phi$ is the phase mismatch parameter of the interaction. This parameter results from an offset from the phase-matching conditions of the acoustic frequency, the optical wavelength, or the incident angle. To analyse the consequences of the phase mismatch alone, we can choose $P/P_0=1$.

Using the efficiency expression (1), it is possible to determine the evolution of the efficiencies for the interactions (e→o) and (o→e) as a function of frequency, wavelength, or incident angle.

Figure 5 shows the evolution in efficiency as a function of the wavelength (5a.) and the acoustic frequency (5b). In both figures, the wavelength λ_0 = 671 nm is considered. As can be seen, the efficiencies are simultaneously at their maximum for the two types of diffraction only at the DD point and decline rapidly when the conditions depart from synchronism.

Close inspection of Figure 5b highlights that the two types of diffraction have different radio frequency bandwidths with (o→e) being narrower than (e→o). Figure 2 explains the difference in bandwidth: the same variation of K will result in two different offsets from synchronism due to the difference in wave vector loci geometries. The difference in radio frequency bandwidth means that even a slight change in the acoustic frequency causes a relative change in the diffraction efficiencies.

As figures 5a and 5b illustrate the evolution in the efficiency when the interaction parameters are set around the DD point, it is clear that the Double Diffraction phase-matching is the only operating point that ensures the same efficiency for both the polarization states. Hence, the DD point is appropriate for linear polarization analysis when a single wavelength is considered.

Simultaneous diffraction of broadband unpolarized light with a fixed incident angle

When the wavelength of the light beam is changed, it is necessary to modify the frequency and the angle of incidence accordingly to recover the wavelength-sensitive DD point. Nevertheless, in some cases, for instance with a broadband optical source, it is not desirable to continuously change the incident angle while scanning the wavelength over the entire optical band.

We now consider that the incident angle for the entire band is set to the Double Diffraction value for one single wavelength, λ_0, called the central wavelength. Once this angle $\theta_{DD,\lambda 0}$ is set, the double diffraction frequency $f_{DD}(\lambda)$ is no longer optimal for wavelengths λ different from λ_0. Consequently, if the f_{DD} determined for λ is applied, then the efficiencies of the two diffraction types will differ and the measured intensities of the two diffracted light beams will no longer reflect the relative proportion of the linear polarization states of the light source.

Figure 6 illustrates this phenomenon. The evolution of the (e→o) and (o→e) diffraction efficiencies are plotted as a function of the wavelength in the vicinity of λ = 405 nm when the incident angle is chosen for double diffraction at λ_0 = 671 nm and the acoustic frequency used is f_{DD} (λ = 405 nm). In this case, and despite the choice of f_{DD}, the two diffraction efficiencies at λ = 405 nm are significantly different (intersection of the two curves and the red line). However, the efficiencies are identical for another wavelength, which guarantees that an optimal operating condition can be found.

Table 1 presents the diffraction efficiencies for three different wavelengths with a central wavelength of λ_0 = 671 nm. Two operating conditions were evaluated: the first with the selection of the Double Diffraction frequency and the second with the selection

of the optimal frequency. The existence and determination of the optimal frequency are discussed in the next section.

From table 1 it is obvious that the (e→o) and (o→e) diffraction efficiencies obtained with the Double Diffraction frequency chosen remain close to each other in the vicinity of λ_0 but become very different when considering wavelengths that are not within the vicinity of λ_0. A ratio of more than 2 exists between the two efficiencies for wavelengths close to the UV band (at 405 nm for example). Such a huge difference confirms that the choice of f_{DD} is not applicable for wideband equal-efficiency diffraction with a fixed incident angle, and consequently, nor for wideband linear polarization analysis. Such applications would benefit from optimized operating conditions to keep diffraction efficiencies constant even when not within the vicinity of λ_0.

Next, we present a method that enables equal diffraction efficiency to be maintained over a wide band with a fixed incident angle, thanks to the choice of an optimal acoustic frequency.

Wideband simultaneous diffraction analysis

For use with a single wavelength, the analysis of linear polarization is simple: the incident angle and the acoustic frequency of the system are set according to the double diffraction point: ($f_{DD}(\lambda)$, $\theta_{DD}(\lambda)$), as explained in section 2. For a small wavelength shift from DD conditions, the differences are relatively negligible if f_{DD} is still used. However, for a wideband polychromatic light beam, the DD conditions are too different from one wavelength to another across the entire band (for example, the entire visible band), as explained in section 3. We analyse hereinafter this issue and show that it is possible to obtain the same efficiencies for both diffraction types with a proper operating frequency strategy, which requires no realignment and with quasi-phase-

matching leading to high efficiency.

First, the incident angle for each simulation was set to $\theta_{DD}(\lambda_0 = 671$ nm) in the context of wideband use of the system across the 400 nm to 700 nm band. We examined the evolution in efficiency as a function of the operating radio frequency and developed a strategy ensuring equal efficiency for both diffraction cases. Indeed, there is still a frequency for which the diffraction efficiency is the same for both the polarization states, even when a wavelength other than λ_0 is chosen. The procedure to derive this frequency was initially developed for double pass systems [18] and was adapted as follows. We set a wavelength λ out of the vicinity of λ_0 and determined the phase mismatch factor $\Delta\Phi$ as a function of the radio frequency for the two diffraction cases in the vicinity of f_{DD}. We calculated the corresponding diffraction efficiencies using (1), determined the relative efficiencies (simply the ratio of (e→o) and (o→e) efficiencies), and identified the frequency necessary to obtain a unity ratio. Figure 7 depicts the evolution of the relative efficiencies as a function of the acoustic frequency for $\lambda = 405$ nm.

As shown in figure 7, the two curves intersect; there is a frequency for which the efficiencies are equal, leading to relative efficiencies equal to unity. The choice of this specific frequency for a wavelength λ corresponds to an optimal choice, $f_{opt,}(\lambda)$, as it ensures equal efficiency for the two diffraction cases without the need for realignment. The choice of the optimal operating frequencies enables the analysis of a linearly polarized light source over a broad bandwidth. Once a practical value of λ_0 was set, the procedure to determine the optimal frequencies was performed numerically for every wavelength λ across the entire band of interest: 400 nm to 700 nm. The evolution of $f_{opt,}$ is presented as a function of λ in figure 8.

Figure 9 compares the relative efficiencies of the interactions for the two operating frequency strategies: f_{DD} and f_{opt}, in the case of a fixed incident angle. The relative efficiency is 1 when the interactions present the same efficiencies, i.e. when $\eta(e \rightarrow o) = \eta(o \rightarrow e)$. As expected, this is the case when the chosen operating frequency strategy corresponds to the optimal frequency f_{opt}. From the curves, it can be seen that for higher wavelengths ($\lambda > 550$ nm), the efficiencies are very close whatever the operating strategy used, as the frequencies f_{DD} and f_{opt} are close to each other in the vicinity of λ_0, making the efficiency error relatively small. However, for lower wavelengths the efficiencies obtained with f_{DD} are different. Indeed, for example at $\lambda =$ 405 nm, there is a ratio of less than 0.4 between the efficiencies when the double diffraction frequency is chosen. Hence, for lower wavelengths, the use of f_{DD} is not valid to obtain equal diffraction efficiency for the two polarization states when analysing unpolarized light over a broad bandwidth. Contrariwise, with the optimal operating frequency strategy presented, this capability is maintained across the entire wavelength range.

We then investigated the influence of the choice of central wavelength λ_0 on efficiency. As an example, with $\lambda_0 = 671$ nm, the efficiency curves in figure 6 intersect at an equal efficiency of 0.13. However, is it possible to obtain a higher value with a different central wavelength for alignment? The answer can be found by studying the evolution of the efficiency (equal efficiency) for several central wavelengths. This evolution is plotted in figure 10. Each one of the curves depicted corresponds to the optimal frequency strategy when $f_{opt}(\lambda)$ is recalculated to satisfy equal efficiency phase-matching for each λ_0 under consideration. Figure 10 shows that an alignment at $\lambda_0 = 437$ nm is very efficient. When the system is aligned at this central wavelength, both polarization states are diffracted with an equal efficiency higher than 0.84 over the

entire visible band. Finally, it can be noted that the practical implementation of the strategy presented is compatible with modern programmable radio frequency generators based on Direct Digital Synthesis (DDS). The transposition to higher wavelength bands is also possible, which would result in a higher overall efficiency thanks to reduced birefringence.

Conclusion

The use of Acousto-Optic Tuneable Filters for the simultaneous diffraction of wideband unpolarized light has been presented. AOTFs can be used under the usual synchronism condition at the Double Diffraction point over a limited optical band. Herein, we have shown that they can also be used with equal efficiency over a wide bandwidth thanks to optimal operating radio frequency conditions. The usual procedure requires the realignment of the setup for each wavelength, whereas we have studied optimal conditions to avoid the need for realignment. We have presented the evolution of the radio frequency needed to maintain equal diffraction efficiencies for both polarization states over a wide bandwidth and the choice of an appropriate central wavelength for alignment. Under such conditions, diffraction of unpolarized light is possible over the entire visible band with quasi-phase matching leading to high efficiency for both polarization states. This can be useful for evaluating linear polarization.

References:

[1] P. R. Kaczmarek, T. Rogowski, A.J. Antonczak, and K. M. Abramski, “Laser Doppler vibrometry with acoustooptic frequency shift,” *Optica Applicata*, vol. 34, no. 3, pp. 373–384, (2004).

[2] V. B. Voloshinov and V. Y. Molchanov, “Acousto-optical modulation of radiation with arbitrary polarization direction,” *Optics & Laser Technology*, vol. 27, no. 5, pp. 307–313, (1995).

[3] D. Trypogeorgos, T. Harte, A. Bonnin, and C. Foot, “Precise shaping of laser light by an acousto-optic deflector,” *Optics Express*, vol. 21, no. 21, p. 24837, (2013)

[4] Li, T., Pareja, J., Becker, L., Heddrich, W., Dreizler, A., & Böhm, B. Quasi-4D laser diagnostics using an acousto-optic deflector scanning system. Applied Physics B, 123(3), 78 (2017)

[5] KB.Yushkov, Va.Molchanov. Acousto-optic filters with arbitrary spectral transmission, Optics Communications, vol. 355, p. 177-180, (2015)

[6] O. Kozlova, A. Sadouni, D. Truong, S. Briaudeau, M. Himbert, Tunable transportable spectrometer based on an acousto-optical tunable filter: Developpement and optical performance, *Review of Scientific Instruments*, 87, 125101 (2016)

[7] Kastelik, J. C., Dupont, S., Benaissa, H., & Pommeray, M. (2006). Bifrequency acousto-optic beam splitter. *Review of scientific instruments*, 77(7), 075103.

[8] Caucheteur, C.; Guo, T.; Albert, J. Polarization-Assisted Fiber Bragg Grating Sensors:Tutorial and Review. *J. Lightwave Technol.*,35, 3311–3322 (2017)

[9] Levenson, M.D., Eesley, G.L. Polarization selective optical heterodyne detection for dramatically improved sensitivity in laser spectroscopy. *Appl. Phys.* 19, 1–17 (1979)

[10] Yan, L., Li, Y., Chandrasekar, V., Mortimer, H., Peltoniemi, J., & Lin, Y. (2020). General review of optical polarization remote sensing. *International Journal of Remote Sensing*, *41*(13), 4853-4864.

[11] Antonov, S.N. Wide-Angle Polarization-Independent Paratellurite-Based Acousto-Optic Laser Radiation Modulator. *Acoust. Phys.* 66, 5–11 (2020)

[12] V. B. Voloshinov, V. Y. Molchanov, and J. C. Mosquera, "Spectral and polarization analysis of optical images by means of acousto-optics," *Optics & Laser Technology*, vol. 28, no. 2, pp. 119–127, (1996).

[13] Sergey P. Anikin, Alexander I. Chizhikov, Vladimir Y. Molchanov, Konstantin B. Yushkov, "AOTF transmission shaping for spectral polarimetric imaging," Proc. SPIE 11525, *SPIE Future Sensing Technologies*, 115251C (8 November 2020)

[14] Obata, R., Yoshinaga, A., Yamamoto, M. et al. Imaging of a retinal pigment epithelium aperture using polarization-sensitive optical coherence tomography. *Jpn J Ophthalmol* (2020)

[15] L.-J. Cheng and G. F. Reyes, "AOTF polarimetric hyperspectral imaging for mine detection," presented at the Detection Technologies for Mines and Minelike Targets, (1995), vol. 2496, pp. 305–311.

[16] E. Dekemper *et al.*, "ALTIUS: a spaceborne AOTF-based UV-VIS-NIR hyperspectral imager for atmospheric remote sensing," (2014), p. 92410L.

[17] G. Rondeaux and M. Herman, "Polarization of light reflected by crop canopies," *Remote Sensing of Environment*, vol. 38, no. 1, pp. 63–75, (1991).

[18] J. Champagne, J.-C. Kastelik, S. Dupont, and J. Gazalet, "Study of the spectral bandwidth of a double-pass acousto-optic system", *Applied Optics*, vol. 57, no. 10, p. C49, (2018).

[19] K. A. McCarthy, A. P. Goutzoulis, M. Gottlieb, and N. B. Singh, “Optical rotatory power in crystals of the mercurous halides and tellurium dioxide,” Optics Communications, vol. 64, no. 2, pp. 157–159, (1987).

Table 1. Diffraction efficiencies as a function of frequency for incident an angle equal to θ_{DD} (λ_0 = 671 nm).

Wavelengh	Non optimised (double diffraction frequency)				Optimised for ϑ_i = ϑ_{DD}(671 nm)	
Λ	f_{DD}	$\eta_{e\to o}$	$\eta_{o\to e}$	E	f_{opt}	$\eta_{e\to o}$=$\eta_{o\to e}$
[nm]	[MHz]	%	%	%	[MHz]	%
671 (λ_0)	87,23	100	100	0	87,23	100
532	116,27	98	98,3	0,3	116,27	98,2
405	174,19	20,7	10	10,7	174,21	53,2

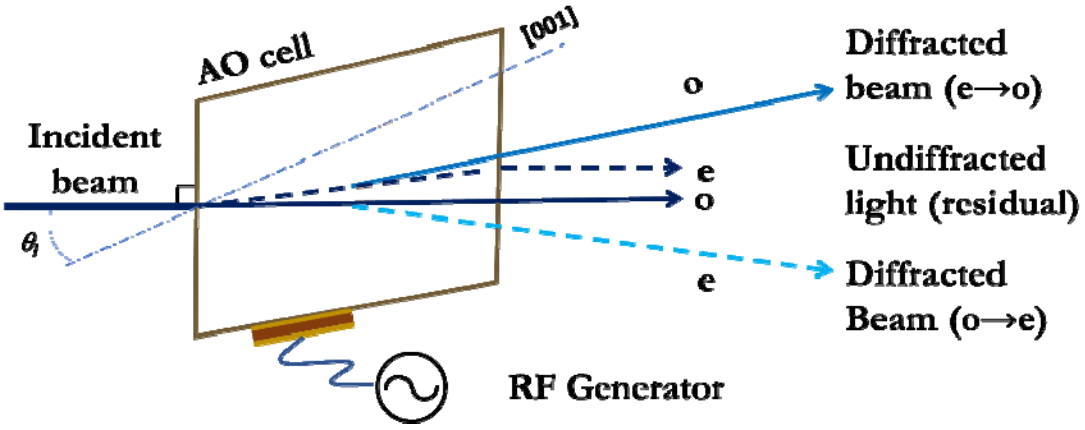

Figure 1. Scheme of an AOTF and double diffraction of a light beam.

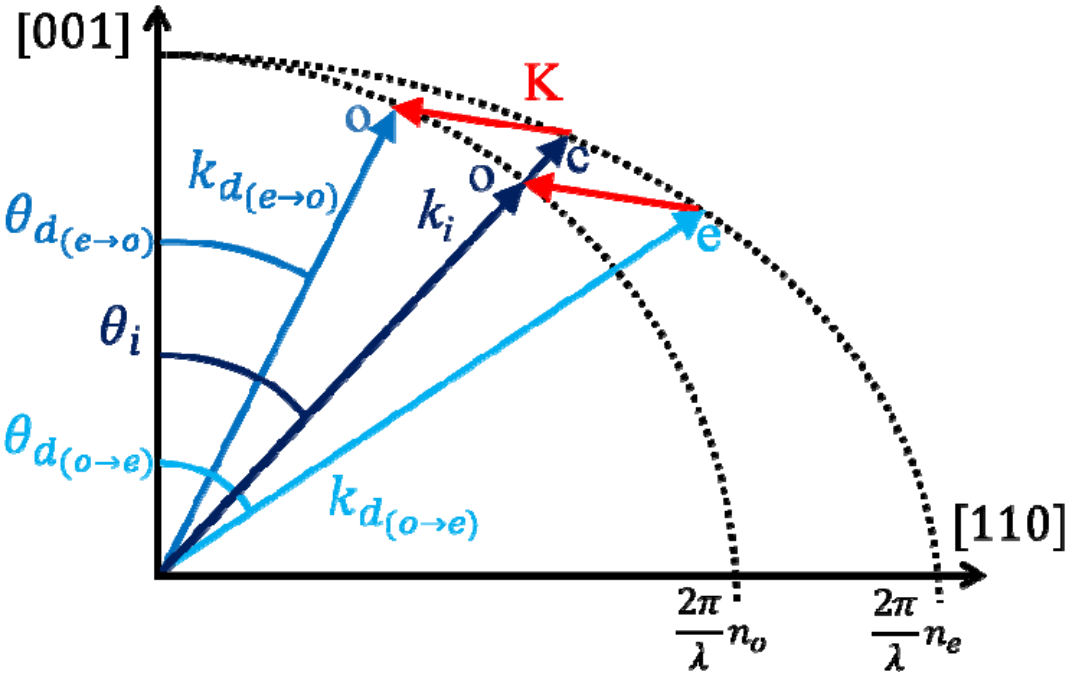

Figure 2. Vector diagram of (e⟶o) and (o⟶e) interactions simultaneously at synchronism. Wave vectors are represented in blue (light blue for diffracted optical beams, dark blue for incident beam) and red for acoustic. Dotted lines represent the wave vectors loci.

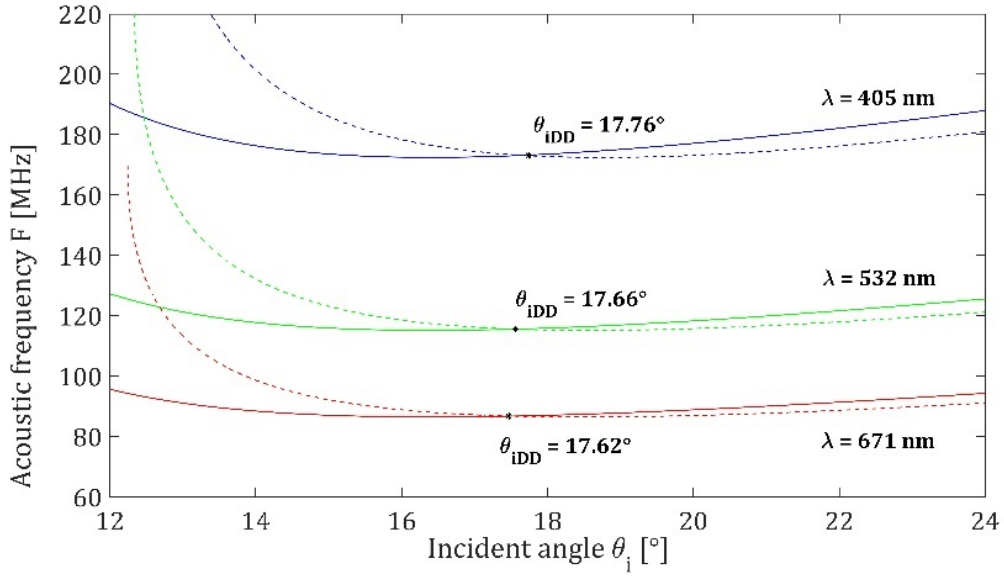

Figure 3. Interaction frequencies at synchronism as a function of incident angle for three wavelengths, solid line o->e case; dashed line e->o case. The double diffraction point are highlighted on the graphs. The acoustic cut is $\theta_a = 8°$.

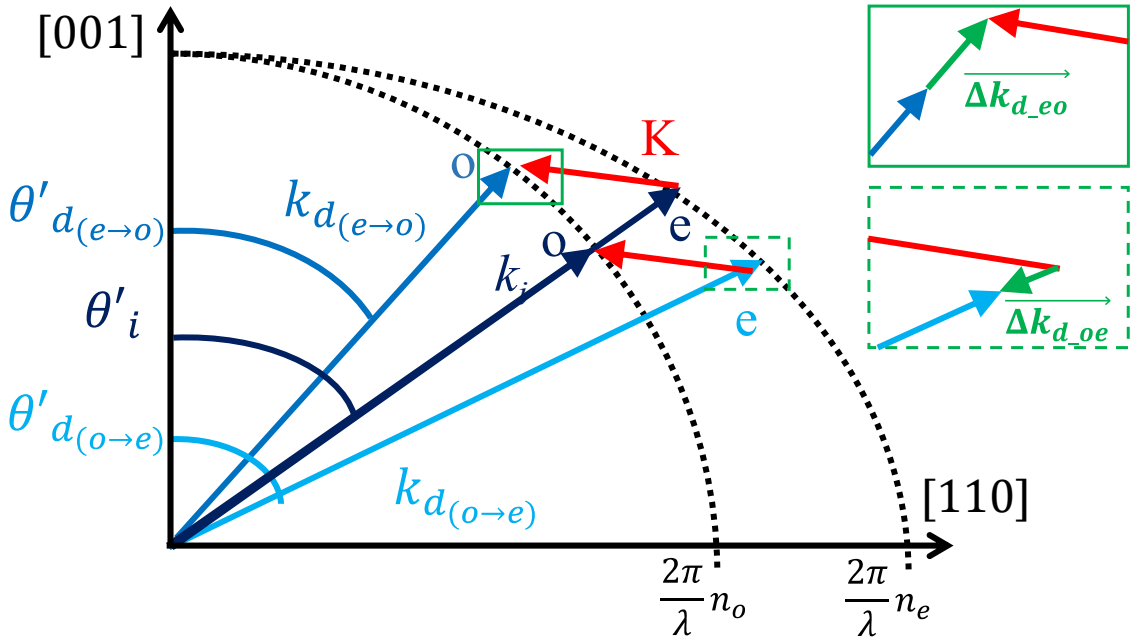

(a)

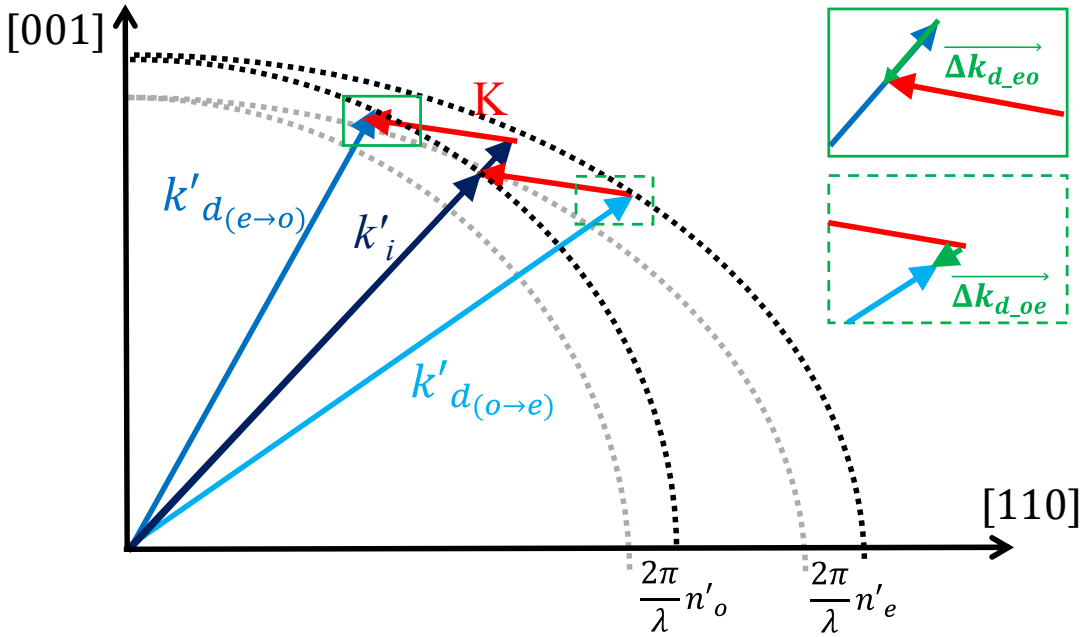

(b)

Figure 4. Vector diagram of (e→o) and (o→e) interactions when synchronism conditions are not met; the momentum mismatch, *Δk*, results from: (a) an offset from the Bragg angle of incidence; (b) *Δk* results from a change in the optical wavelength which modifies the wave vector loci.

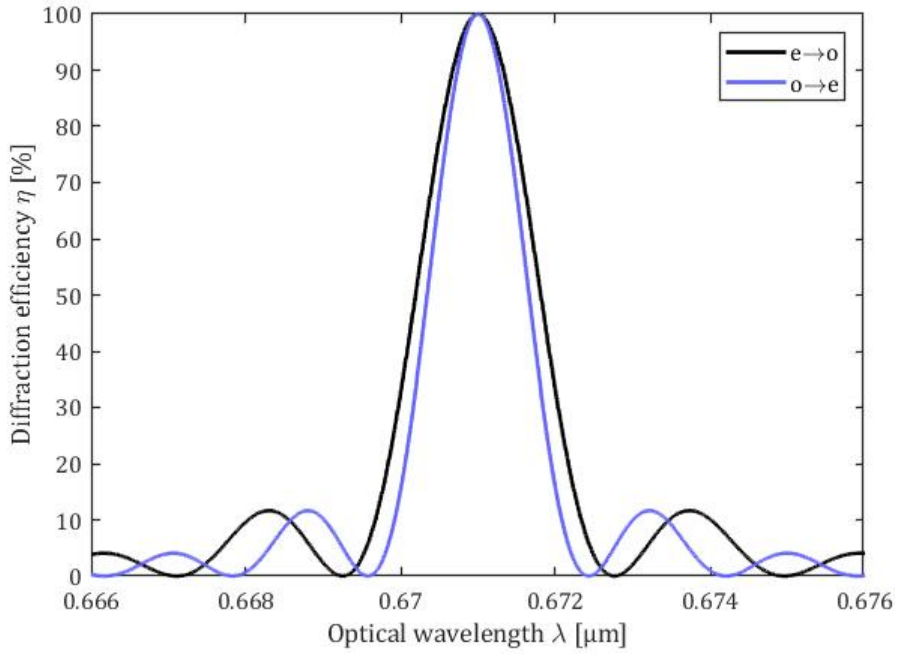

(a)

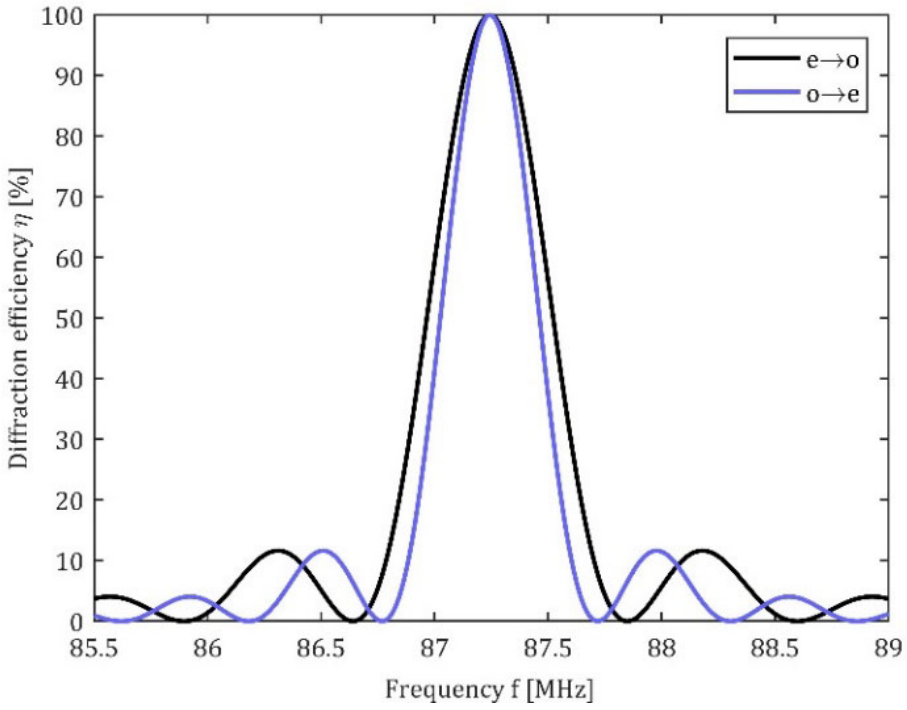

(b)

Figure 5. Evolution of the two diffraction type efficiencies with $\theta = \theta_{DD}$ for $\lambda_0 = 671$ nm; (a) as a function of wavelength when $f = f_{DD}$. The efficiencies are maximum for $\lambda = \lambda_0$; and (b) as a function of acoustic frequency when $\lambda = \lambda_0$. The efficiencies are maximum when $f = f_{DD}$.

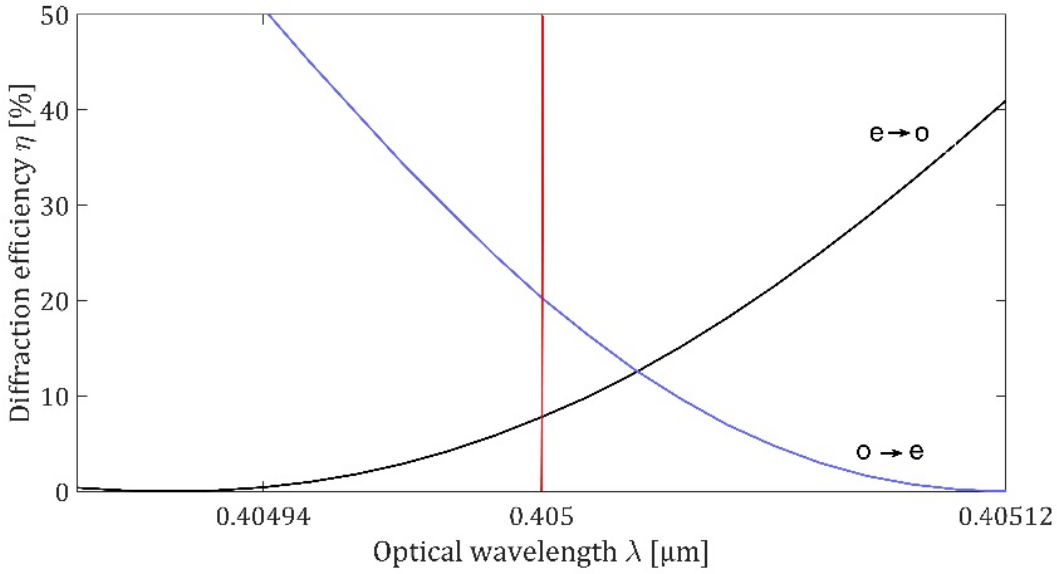

Figure 6. Diffraction efficiency evolution for the two interaction types as a function of λ, for θ_{DD} (λ_0 = 671 nm) and f_{DD} (λ = 405 nm).

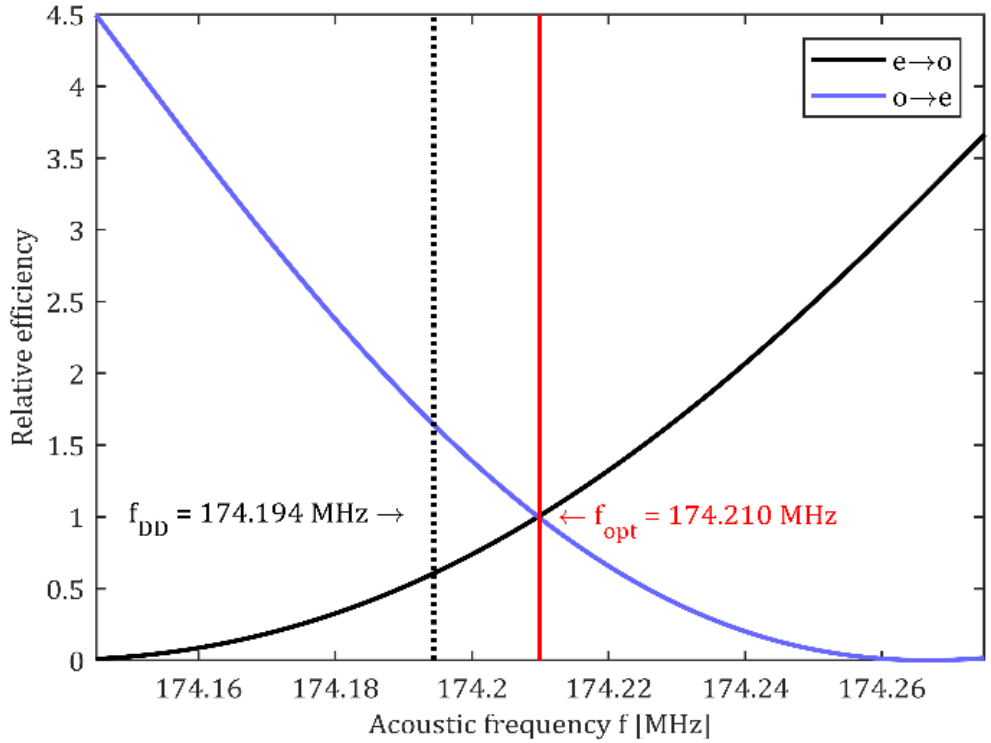

Figure 7. Relative efficiency of the interactions for λ = 405 nm as a function of the acoustic frequency, with $\theta = \theta_{DD}(\lambda_0 = 671$ nm). f_{DD} and f_{opt} are highlighted.

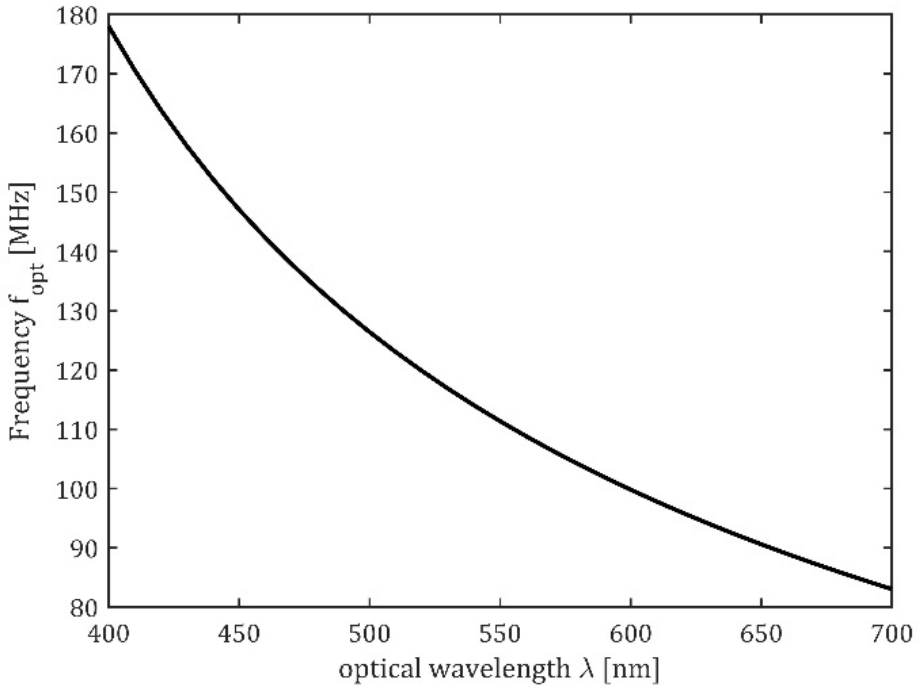

Figure 8. Optimal frequencies, $\theta_i = \theta_{DD}$ (λ_0 = 671 nm) and θ_a =8°.

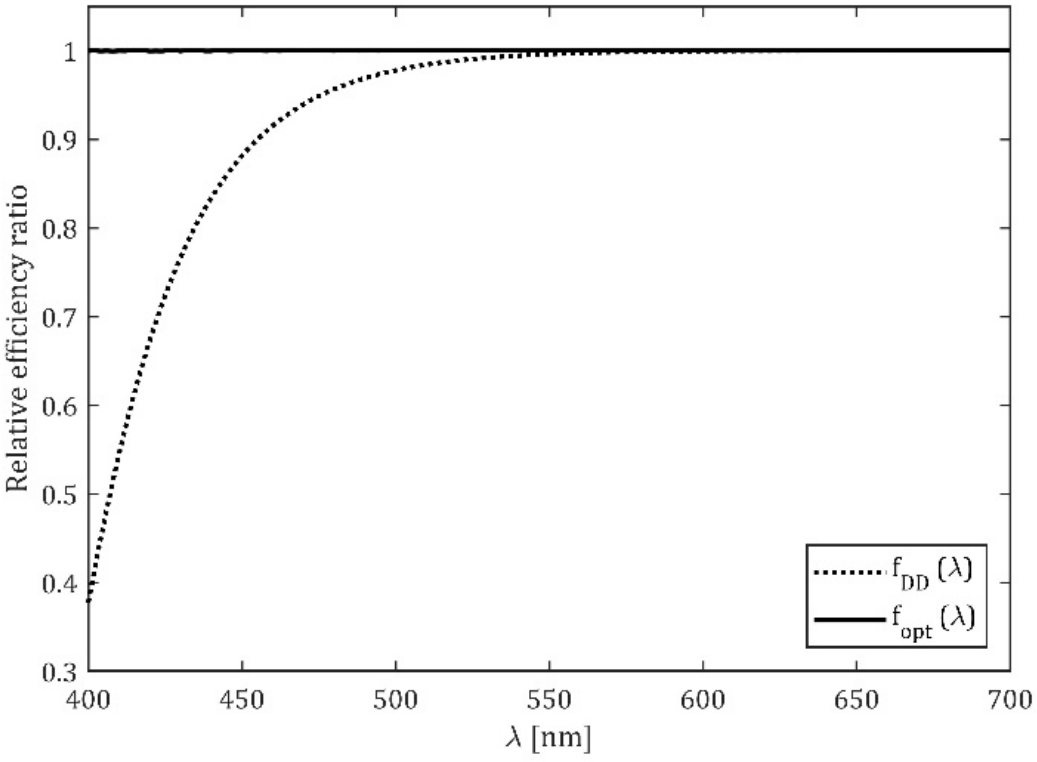

Figure 9. Relative efficiency evolution for the Double Diffraction frequency strategy and the optimal frequency strategy, as a function of wavelength. λ_0 = 671 nm.

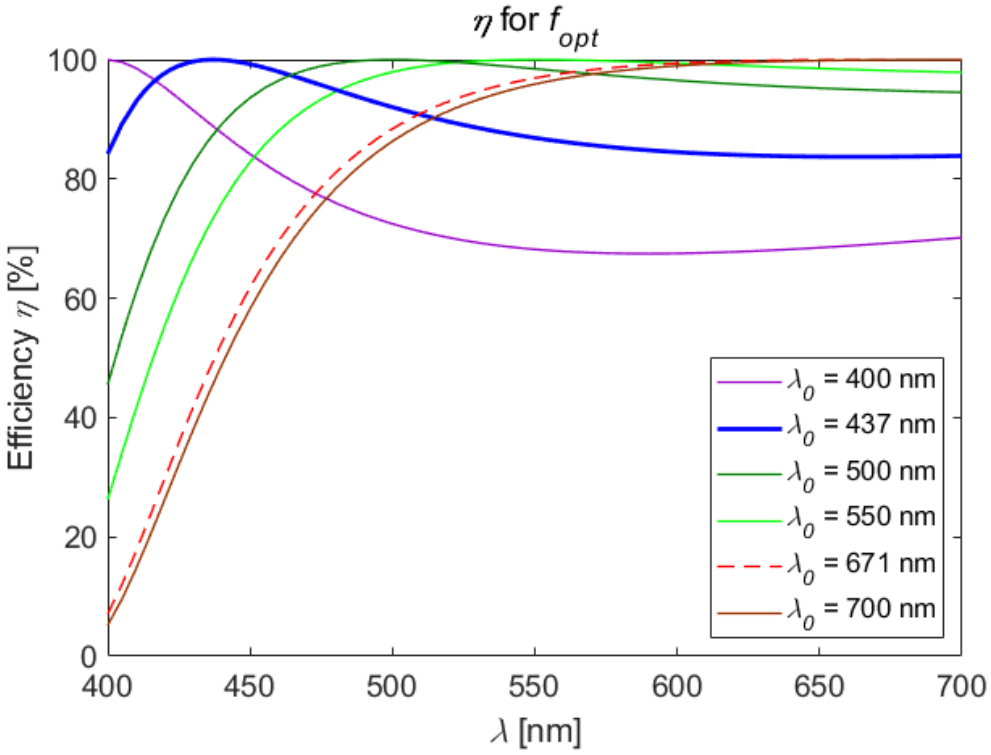

Figure 10. Evolution of the efficiency for the optimal frequency strategy, as a function of wavelength, for different values of central wavelength λ_0.